

# Statistical Mechanical Approach to Phase Unwrapping in Remote Sensing Using the Synthetic Aperture Radar Interferometry

Yohei SAIKA<sup>1,\*</sup> and Tatsuya UEZU<sup>2</sup>

<sup>1</sup>*Department of Information and Computer Engineering, Gunma National College of Technology,  
Maebashi 371-8530, Japan*

<sup>2</sup>*Department of Physics, Nara Women's University, Nara 630-8506, Japan*

Received April 19, 2013; final version accepted June 10, 2013

On the basis of analogy between Bayesian inference and statistical mechanics, we construct a method of wave-front reconstruction in remote sensing using the synthetic aperture radar (SAR) interferometry. Here, we use the maximizer of the posterior marginal (MPM) estimate for phase unwrapping and maximum entropy for noise reduction from unwrapped wave-fronts. Next, we investigate static property of the MPM estimate from a phase diagram described by using Monte Carlo simulation for a wave-front which is typical in remote sensing using the SAR interferometry. The phase diagram clarifies that phase unwrapping is accurately realized by the MPM estimate using an appropriate model prior under the constraint of surface-consistency condition, and that the MPM estimate smoothly carries out phase unwrapping utilizing fluctuations around the MAP solution. Also, using the Monte Carlo simulations, we clarify that the method of maximum entropy using an appropriate model prior succeeds in reducing noises from the unwrapped wave-front obtained by the MPM estimate.

**KEYWORDS:** statistical mechanics, Bayesian inference, phase unwrapping, Monte Carlo simulation, phase diagram

## 1. Introduction

Wave-fronts have been often carrying information through noisy channel. Numerous researchers [1–10] have investigated methodologies of utilizing information on the wave-fronts both from theoretical and practical viewpoints. Also, they have constructed information technology [1] to reconstruct an original wave-front from an interferogram observed by optical instruments using the interferometer. This problem has been called as phase unwrapping and then a lot of techniques have been proposed to solve this problem, such as least squares estimation [2–6], the MAP estimation using the conjugate gradient method [7], the MAP estimation using simulated annealing [8, 9], the method of maximum entropy [9] and Edgelist phase unwrapping algorithm for time series InSAR analysis [10]. Although the MAP estimation using simulated annealing [8, 9] was tried for this problem, there have been few systematic approaches for clarifying both static and dynamic properties of phase unwrapping based on the Bayesian inference using the maximizer of the posterior marginal (MPM) estimate. On the other hand, in recent years, theoretical physicists have investigated problems of information science, such as image restoration and error-correcting codes on the basis of an analogy between statistical mechanics and Bayesian inference using the MPM estimate [11–14]. Statistical mechanics has then been applied to information technology, such as information communication [15] and quantum computation [16]. Then, the field of statistical mechanics of information has been developed as an established research field called as statistical mechanical informatics [13, 14]. One of the present authors (Y.S.) have investigated problems of image restoration using the plane rotator model [17], inverse halftoning [18, 19] and phase retrieval [20]. Though phase retrieval was investigated via the statistical mechanics of the Q-Ising model by Saika and Nishimori [20], however, they treated this problem under a restricted condition.

Therefore, in this study, on the basis of the analogy between statistical mechanics and Bayesian inference, we construct a method of wave-front reconstruction in remote sensing using the SAR interferometry. For this purpose, we first carry out phase unwrapping using the MPM estimate corresponding to the statistical mechanics of a three-state Ising model. Here, we use the model prior which suppresses the number of non-zero states of the three-state Ising spin at each sampling point. Then, we use the likelihood composed of two terms: one is the term that enhances smooth structures in wave-fronts and the other is a surface-consistency condition of the wave-fronts. In the next procedure, we carry out noise reduction using the method of maximum entropy. Next, in order to clarify performance of the present

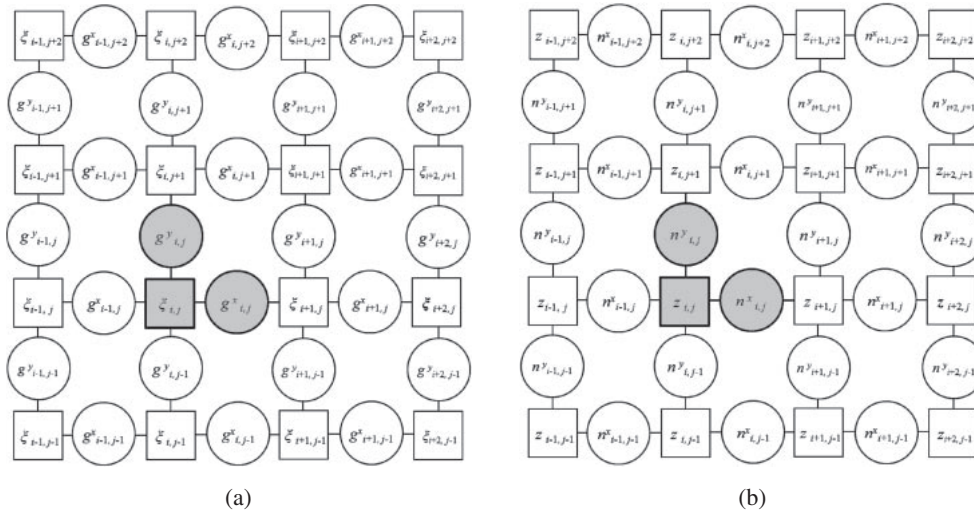


Fig. 1. (a) Lattice points where the original wave-front, the interferogram and the set of phase differences are arranged. (b) Lattice points where both the three-state Ising model and the reconstructed wave-front are arranged.

method from the viewpoint of statistical mechanics, we utilize Monte Carlo simulations for a wave-front which is typical in remote sensing using the SAR interferometry. Although the performance is estimated for a single artificial wave-front, we expect that this model has general property of wave-fronts in remote sensing using the SAR interferometry. First, we estimate the static property of the MPM estimate for phase unwrapping from a phase diagram representing the stability of a PU phase in the hyper-parameter space. The term ‘‘PU phase’’ is used here to represent a domain in which the MPM estimate succeeds in phase unwrapping with high degree of accuracy in the hyper-parameter space. The phase diagram clarifies that the MPM estimate accurately reconstructs the original wave-front using the appropriate model prior enhancing smooth structures under the constraint of the surface-consistency condition at each plaquette. Also, we find that the method of maximum entropy succeeds in noise reduction using the appropriate model of the true prior enhancing smooth structures in wave-fronts.

The content of this manuscript is organized as follows. First, we show a general formulation for the problem of wave-front reconstruction composed of phase unwrapping due to the MPM estimate and noise reduction due to the method of maximum entropy. Then, we investigate the performance of the present method using the Monte Carlo simulation for the artificial and typical wave-front in remote sensing using the SAR interferometry. Last part is devoted to summary and discussion.

## 2. General Formulation

In this chapter, we indicate the general formulation for the problem of wave-front reconstruction using the MPM estimate for phase unwrapping and the maximum entropy for noise reduction.

Let us first consider an original wave-front  $\{\xi_{i,j}\}$  ( $0 < \xi_{i,j} < \infty$ ,  $i, j = 1, \dots, L$ ) arranged on the square lattice in Fig. 1(a). If we treat a realistic case, we use a realistic wave-front in Fig. 2(a) in remote sensing using the SAR interferometry. On the other hand, if we investigate statistical performance of the present method, we need to consider a set of wave-fronts  $\{\xi_{i,j}\}$  that are generated by the true prior expressed as  $\Pr(\{\xi_{i,j}\})$ . Then, as shown in Fig. 2(b), the original wave-front is corrupted into the noisy corrupted one:

$$\eta_{i,j} = \xi_{i,j} + n_{i,j}^a \quad (2.1)$$

by some noise  $\{n_{i,j}^a\}$ . In this study, we assume the Gaussian noise  $N(0, \sigma_a^2)$  onto the corrupted wave-front at each site. Here,  $\sigma_a^2$  is variance of the Gaussian noise. We note that difference between the original and corrupted wave-fronts is not clearly seen from Figs. 2(a) and 2(b), as the variance of the Gaussian noise is set to be small, i.e.,  $\sigma_a^2 = 0.01$ . Then, as seen from Fig. 2(c), we observe an interferogram:

$$g_{i,j} = \text{mod}(\eta_{i,j} + \pi, 2\pi) - \pi \quad (2.2)$$

using the optical instruments due to the interferometer. Then, we derive two sets of phase differences:

$$g_{i,j}^x = \text{mod}(g_{i+1,j} - g_{i,j} + n_{i,j}^{bx} + \pi, 2\pi) - \pi \quad (2.3)$$

and

$$g_{i,j}^y = \text{mod}(g_{i,j+1} - g_{i,j} + n_{i,j}^{by} + \pi, 2\pi) - \pi \quad (2.4)$$

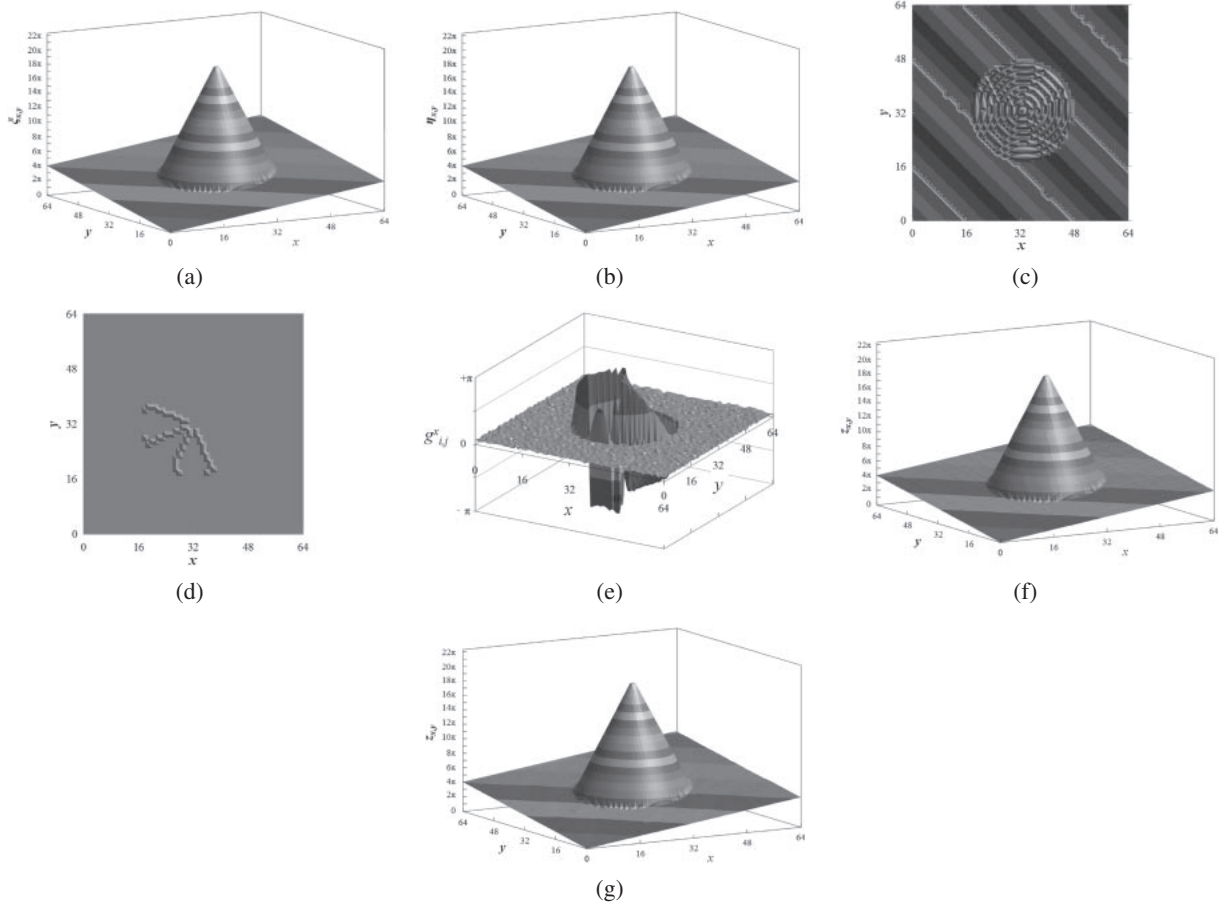


Fig. 2. (a) An original wave-front often used in remote sensing using the SAR interferometry. (b) A wave-front corrupted by the Gaussian noise ( $\sigma_a = 0.01$ ) from the original wave-front of (a). (c) An interferogram of the corrupted wave-front of (b) observed by the interferometer. (d) A residue pattern of the interferogram of (c). (e) A set of corrupted phase differences in a principal interval derived from the interferogram in (c). (f) A wave-front obtained by the MPM estimate for phase unwrapping, if we set to  $J = 1$ ,  $\Gamma = 1$ ,  $h = 1$ , and  $T_m = 3.5$  ( $\sigma = 2.6239$ ). (g) A wave-front obtained by the method of maximum entropy from the unwrapped wave-front in (f), if we set to  $J_n = 1$ ,  $\Gamma_n = 10$ ,  $h_n = 10$ , and  $T_n = 1.0$  ( $\sigma = 1.7034$ ).

in the principal interval from  $-\pi$  to  $+\pi$ . These phase differences in Fig. 2(d) are corrupted by some noises  $\{n_{i,j}^{bx}\}$  and  $\{n_{i,j}^{by}\}$ . In this study, we assume the Gaussian noise  $N(0, \sigma_b^2)$  for  $\{n_{i,j}^{bx}\}$  and  $\{n_{i,j}^{by}\}$ . Here, as seen from the Nyquist sampling theorem, if absolute value of wave-front slope is less than  $\pi$ , such as

$$|\eta_{i+1,j} - \eta_{i,j}| < \pi, \quad (2.5)$$

at each neighboring sampling point, then the wave-front  $\{\eta_{i,j}\}$  is completely determined by sampling. Otherwise, if the absolute values of wave-front slopes are more than  $\pi$ , such as

$$|\eta_{i+1,j} - \eta_{i,j}| > \pi, \quad (2.6)$$

at several neighboring sampling points, then the wave-front  $\{\eta_{i,j}\}$  is not determined due to aliasing. In this case, there appear residues in the pattern of the interferogram in Fig. 2(d). Then, as shown in Fig. 2(e), discontinuity appears at several sampling points in the pattern of phase differences  $\{g_{i,j}^x\}$  and  $\{g_{i,j}^y\}$  restricted to the principal interval.

Next, we carry out phase unwrapping by using the sets of principal phase differences  $\{g_{i,j}^x\}$  ( $|g_{i,j}^x| < \pi$ ,  $i = 1, \dots, L-1$ ,  $j = 1, \dots, L$ ) and  $\{g_{i,j}^y\}$  ( $|g_{i,j}^y| < \pi$ ,  $i = 1, \dots, L$ ,  $j = 1, \dots, L-1$ ) based on the Bayesian inference using the MPM estimate corresponding to statistical mechanics of the three-state Q-Ising model  $\{n_{i,j}^x\}$  ( $n_{i,j}^x = -1, 0, +1$ ,  $i = 1, \dots, L-1$ ,  $j = 1, \dots, L$ ) and  $\{n_{i,j}^y\}$  ( $n_{i,j}^y = -1, 0, +1$ ,  $i = 1, \dots, L$ ,  $j = 1, \dots, L-1$ ) on the square lattice in Fig. 1(b). Using these model systems, we reconstruct the original wave-front as

$$\hat{n}_{x,y}^x = \arg \max_{\{n_{i,j}^x\} \neq n_{x,y}^x} \sum_{\{n_{i,j}^y\}} \Pr(\{n_{i,j}^x\}, \{n_{i,j}^y\} | \{g_{i,j}^x\}, \{g_{i,j}^y\}) \quad (2.7)$$

and

$$\hat{n}_{x,y}^y = \arg \max_{\{n_{i,j}^y\} \neq n_{x,y}^y} \sum_{\{n_{i,j}^x\}} \Pr(\{n_{i,j}^x\}, \{n_{i,j}^y\} | \{g_{i,j}^x\}, \{g_{i,j}^y\}). \quad (2.8)$$

Here, the posterior probability is estimated based on the Bayes' formula:

$$\Pr(\{n_{i,j}^x\}, \{n_{i,j}^y\} | \{g_{i,j}^x\}, \{g_{i,j}^y\}) \propto \Pr(\{n_{i,j}^x\}, \{n_{i,j}^y\}) \Pr(\{g_{i,j}^x\}, \{g_{i,j}^y\} | \{n_{i,j}^x\}, \{n_{i,j}^y\}), \quad (2.9)$$

using the model of the true prior and the likelihood. In this study, we assume the model of the true prior which enhances smooth structures as

$$\Pr(\{n_{i,j}^x\}, \{n_{i,j}^y\}) \propto \exp\left[-\frac{1}{T_m} E_p(\{n_{i,j}^x\}, \{n_{i,j}^y\})\right], \quad (2.10)$$

where

$$E_p(\{n_{i,j}^x\}, \{n_{i,j}^y\}) = h \sum_{(i,j)} (|n_{i,j}^x| + |n_{i,j}^y|) \quad (2.11)$$

which is the cost-function representing prior information so as to suppress occurrence of residues in the reconstructed wave-fronts. Then, we assume the likelihood as

$$\Pr(\{g_{i,j}^x\}, \{g_{i,j}^y\} | \{n_{i,j}^x\}, \{n_{i,j}^y\}) \propto \exp\left[-\frac{1}{T_m} (E_{11}(\{g_{i,j}^x\}, \{g_{i,j}^y\} | \{n_{i,j}^x\}, \{n_{i,j}^y\}) + E_{12}(\{g_{i,j}^x\}, \{g_{i,j}^y\} | \{n_{i,j}^x\}, \{n_{i,j}^y\}))\right] \quad (2.12)$$

where the cost-functions representing the likelihood are assumed as

$$\begin{aligned} E_{11}(\{g_{i,j}^x\}, \{g_{i,j}^y\} | \{n_{i,j}^x\}, \{n_{i,j}^y\}) \\ = J \sum_{(i,j)} \left( n_{i+1,j}^x - n_{i,j}^x + \frac{1}{2\pi} (g_{i+1,j}^x - g_{i,j}^x) \right)^2 + J \sum_{(i,j)} \left( n_{i,j+1}^y - n_{i,j}^y + \frac{1}{2\pi} (g_{i,j+1}^y - g_{i,j}^y) \right)^2 \\ + J \sum_{(i,j)} \left( n_{i+1,j}^y - n_{i,j}^y + \frac{1}{2\pi} (g_{i+1,j}^y - g_{i,j}^y) \right)^2 + J \sum_{(i,j)} \left( n_{i,j+1}^x - n_{i,j}^x + \frac{1}{2\pi} (g_{i,j+1}^x - g_{i,j}^x) \right)^2 \end{aligned} \quad (2.13)$$

and

$$\begin{aligned} E_{12}(\{g_{i,j}^x\}, \{g_{i,j}^y\} | \{n_{i,j}^x\}, \{n_{i,j}^y\}) \\ = (2\pi)^2 \Gamma \sum_{(i,j)} \left( n_{i,j}^x + n_{i+1,j}^y - n_{i,j+1}^x - n_{i,j}^y + \frac{1}{2\pi} (g_{i,j}^x + g_{i+1,j}^y - g_{i,j+1}^x - g_{i,j}^y) \right)^2. \end{aligned} \quad (2.14)$$

In above equations,  $J$ ,  $h$ ,  $\Gamma$ , and  $T_m$  are hyper-parameters which we should determine to carry out Bayesian inference. As seen from Eq. (2.13), the former term in the light-hand side of Eq. (2.12) is assumed to enhance smooth structures in the pattern of wave-fronts. Then, as seen from Eq. (2.14), the latter term in the light-hand side of Eq. (2.12) is introduced so as to satisfy the constraint of the surface-consistency condition.

Next, using the sets of  $\{\hat{n}_{i,j}^x\}$  and  $\{\hat{n}_{i,j}^y\}$ , we then reduce noises by the method of maximum entropy from the reconstructed wave-front. Here, using the model systems  $\{\theta_{i,j}^x\}$  ( $|\theta_{i,j}^x| < \pi$ ,  $i = 1, \dots, L-1$ ,  $j = 1, \dots, L$ ) and  $\{\theta_{i,j}^y\}$  ( $|\theta_{i,j}^y| < \pi$ ,  $i = 1, \dots, L$ ,  $j = 1, \dots, L-1$ ) we remove noises so as to maximize entropy at finite temperature  $T_n$  for the model system with cost function:

$$\begin{aligned} E(\{\theta_{i,j}^x\}, \{\theta_{i,j}^y\} | \{\hat{n}_{i,j}^x\}, \{\hat{n}_{i,j}^y\}) \\ = E_1(\{\theta_{i,j}^x\}, \{\theta_{i,j}^y\} | \{\hat{n}_{i,j}^x\}, \{\hat{n}_{i,j}^y\}) + E_2(\{\theta_{i,j}^x\}, \{\theta_{i,j}^y\} | \{\hat{n}_{i,j}^x\}, \{\hat{n}_{i,j}^y\}) + E_3(\{\theta_{i,j}^x\}, \{\theta_{i,j}^y\} | \{\hat{n}_{i,j}^x\}, \{\hat{n}_{i,j}^y\}) \end{aligned} \quad (2.15)$$

which is composed of three terms: one is assumed to enhance smooth structures in the pattern of original wave-fronts as

$$\begin{aligned} E_1(\{\theta_{i,j}^x\}, \{\theta_{i,j}^y\} | \{\hat{n}_{i,j}^x\}, \{\hat{n}_{i,j}^y\}) \\ = J_n \sum_{(i,j)} \left( \hat{n}_{i+1,j}^x - \hat{n}_{i,j}^x + \frac{1}{2\pi} (\theta_{i+1,j}^x - \theta_{i,j}^x) \right)^2 + J_n \sum_{(i,j)} \left( \hat{n}_{i,j+1}^y - \hat{n}_{i,j}^y + \frac{1}{2\pi} (\theta_{i,j+1}^y - \theta_{i,j}^y) \right)^2, \end{aligned} \quad (2.16)$$

and second is assumed to satisfy the surface-consistency condition as

$$E_2(\{\theta_{i,j}^x\}, \{\theta_{i,j}^y\} | \{\hat{n}_{i,j}^x\}, \{\hat{n}_{i,j}^y\}) = (2\pi)^2 \Gamma_n \sum_{(i,j)} \left( \hat{n}_{i,j}^x + \hat{n}_{i+1,j}^y - \hat{n}_{i,j+1}^x - \hat{n}_{i,j}^y + \frac{1}{2\pi} (\theta_{i,j}^x + \theta_{i+1,j}^y - \theta_{i,j+1}^x - \theta_{i,j}^y) \right)^2. \quad (2.17)$$

Then, third is assumed to enhance observed phase differences  $\{\tau_{i,j}^x\}$  and  $\{\tau_{i,j}^y\}$  as

$$E_3(\{\theta_{i,j}^x\}, \{\theta_{i,j}^y\} | \{\hat{n}_{i,j}^x\}, \{\hat{n}_{i,j}^y\}) = h_n \sum_{(i,j)} (\theta_{i,j}^x - \tau_{i,j}^x)^2 + h_n \sum_{(i,j)} (\theta_{i,j}^y - \tau_{i,j}^y)^2. \quad (2.18)$$

For this purpose, we carry out the method of maximum entropy using the Monte Carlo simulation at  $T_n (= 1)$ . In above equations,  $J_n$ ,  $\Gamma_n$ ,  $h_n$ , and  $T_n$  are hyper-parameters. Here, we denote the solutions of this method as  $\{\hat{\theta}_{i,j}^x\}$  and  $\{\hat{\theta}_{i,j}^y\}$  and therefore the reconstructed wave-front  $\{z_{i,j}\}$  is denoted as

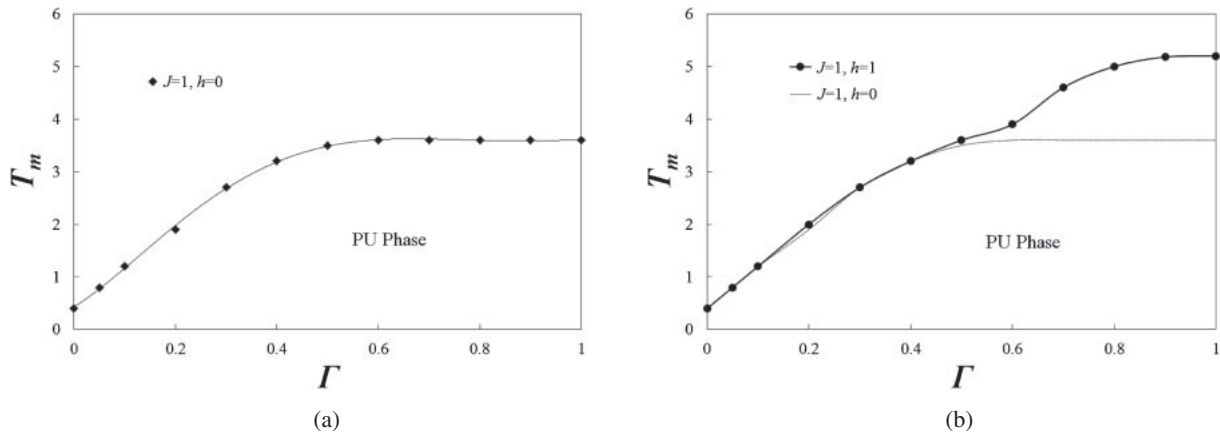


Fig. 3. Phase diagram representing the stability of the PU phase in the hyper-parameter space with respect to the original wave-front in Fig. 2(a). (a) Solid line shows the upper phase boundary of the PU phase along the  $T_m$  axis, if we set to  $J = 1, h = 0$ . (b) Solid line shows the upper phase boundary of the PU phase along the  $T_m$  axis, if we set to  $J = 1, h = 1$ . Dotted line shows the upper phase boundary along the  $T_m$  axis, if  $J = 1, h = 0$ .

$$z_{m,n} = z_{1,1} + \sum_{i=1}^{m-1} (2\pi\hat{n}_{i,1}^x + \hat{\theta}_{i,1}^x) + \sum_{j=1}^{n-1} (2\pi\hat{n}_{m,j}^y + \hat{\theta}_{m,j}^y). \quad (2.19)$$

In this equation, we should estimate a variable  $z_{1,1}$  so as to minimize the mean square error between the original and reconstructed wave-fronts as

$$\sigma = \sum_{m=1}^L \sum_{n=1}^L (z_{m,n} - \xi_{m,n})^2. \quad (2.20)$$

Here, this value takes zero, if the wave-front is reconstructed completely.

### 3. Performance

In this chapter, we investigate the performance of the present method using the Monte Carlo simulation for the wave-front in remote sensing using the SAR interferometry. First, in order to clarify the performance of the MPM estimate for phase unwrapping, we use the original wave-front in Fig. 2(a). Then, the original wave-front is corrupted by the Gaussian noise  $N(0, \sigma_a^2)$  into the noisy corrupted one in Fig. 2(b), if it is transmitted through the noisy channel. Here, the Gaussian noise  $N(0, \sigma_a^2)$  is not clearly seen from Fig. 2(b), because we set to  $\sigma_a = 0.01$ . Then, the receiver observes the interferogram in Fig. 2(c). From this interferogram, we derive the sets of the principal phase differences in Fig. 2(d). Here, we introduce the Gaussian noise  $N(0, \sigma_b^2)$  with  $\sigma_b = 0.3$  into the phase differences. Next, when we carry out phase unwrapping from the interferogram, we use the Monte Carlo simulations with 20000 Monte Carlo steps (MCSs). Here, in order to clarify static property, we display the phase diagram in Fig. 3(a) representing the stability of the PU phase in which the MPM estimate succeeded in phase unwrapping in the  $T_m$ - $\Gamma$  plane. The phase diagram in Fig. 3(a) indicates that the term of the surface-consistency condition plays an important role to extend the PU phase. Then, as shown in Fig. 3(b), we find that introducing the appropriate model prior into the present model is also useful for extending the PU phase under the constraint of the surface-consistency condition. Next, we estimate the dynamic property of the MPM estimate by evaluating time evolution of the mean square error due to the Monte Carlo simulation for the wave-front in Fig. 2(a). Here, the simulations clarify that the MPM estimate reconstructs the original wave-front with up to 100 MCSs utilizing fluctuations around the MAP solution by tuning the parameter  $T_n$  appropriately. Next, we estimate the performance of the method of maximum entropy for noise reduction from the unwrapped wave-front in Fig. 2(e). The reconstructed wave-front in Fig. 2(f) is obtained by using the method of maximum entropy, although the difference between the unwrapped and reconstructed wave-fronts is not clearly seen from Figs. 2(f) and 2(g). However, as seen from these results based on the performance measure via the mean square error, we find that the mean square error of the reconstructed wave-front ( $\sigma = 1.7034$ ) is superior to that of the unwrapped one ( $\sigma = 2.6239$ ). From this fact, we suggest that the method of maximum entropy succeeds in noise reduction from the unwrapped wave-front, if we assume the appropriate model prior.

### 4. Summary and Discussion

In the previous chapters, on the basis of the analogy between statistical mechanics and Bayesian inference, we have constructed the method of wave-front reconstruction both using the MPM estimate for phase unwrapping and the

maximum entropy for noise reduction. Then, we estimated the performance of the present method using the Monte Carlo simulations for the artificial wave-front in remote sensing using the SAR interferometry. For this purpose, we first described the phase diagram to specify the domain where the PU phase was stabilized by the MPM estimate. From this phase diagram, we clarified that the term of the surface-consistency condition played an important role to extend the PU phase and also that introducing the appropriate model prior into the present model was also useful for extending the PU phase under the constraint of the surface-consistency condition. Next, we found that the MPM estimate smoothly reconstructed the original wave-front by making use of the fluctuations around the MAP solution. Further, using the Monte Carlo simulations for the wave-front, we evaluated the performance of the method of maximum entropy for noise reduction from the unwrapped wave-front obtained by the MPM estimate. We found that the noise reduction due to the method of maximum entropy was available of improving the performance of the present method, if we utilized the appropriate model of the true prior.

As a future problem, we are going to construct a practical method for wave-front reconstruction using the techniques established in statistical mechanics, such as the Bethe approximation. Then, we are going to examine the performance of these methods for realistic problems.

#### REFERENCES

- [1] Ghiglia, D. C., and Pritt, M. D., *Two-Dimensional Phase Unwrapping Theory Algorithms and Software*, Wiley, New York (1998).
- [2] Fried, D. L., "Least-square fitting of a wave-front distortion estimate to an array of phase differences measurements," *J. Opt. Soc. Am.*, **67**: 370–375 (1977).
- [3] Hudgin, R. H., "Wave-front reconstruction for compensated imaging," *J. Opt. Soc. Am.*, **67**: 375–378 (1977).
- [4] Noll, R. J., "Phase estimation from slope-type wave-front sensors," *J. Opt. Soc. Am.*, **68**: 139–140 (1978).
- [5] Goldstein, R. M., and Zebker, H. A., "Interferometric radar mapping of ocean currents," *Nature*, **328**: 707–709 (1987).
- [6] Ghiglia, D. C., and Romero, L. A., "Robust two-dimensional weighted and unweighted phase unwrapping that uses fast transforms and iterative method," *J. Opt. Soc. Am. A*, **11**: 107–117 (1994).
- [7] Marroquin, J. L., and Rivera, M., "Quadratic regularization functionals for phase unwrapping," *J. Opt. Soc. Am. A*, **12**: 2393–2400 (1995).
- [8] Guerriero, L., Nico, G., Pasquariello, G., and Stramaglia, R., "A new regularization scheme for phase unwrapping," *Appl. Opt.*, **37(14)**: 3053–3058 (2000).
- [9] Nico, G., Palubinskas, G., and Datcu, M., "Bayesian approaches to phase unwrapping: Theoretical study," *IEEE Trans. Signal-Processing*, **48(4)**: 2545–2556 (2000).
- [10] Shanker, A. P., and Zebker, H., "Edgelist phase unwrapping algorithm for time series InSAR analysis," *J. Opt. Soc. Am. A*, **27(3)**: 605–612 (2010).
- [11] Nishimori, H., and Wong, K. Y. M., "Statistical mechanics of image restoration and error correcting codes," *Phys. Rev. E*, **60**: 132–144 (1999).
- [12] Kabashima, Y., and Saad, D., "Statistical mechanics of error correcting codes," *Europhys. Lett.*, **45**: 97–103 (1999).
- [13] Nishimori, H., *Theory of Spin Glasses and Information; An Introduction*, Oxford, London (2001).
- [14] Tanaka, K., "Statistical mechanical approach to image processing," *J. Phys. A: Mathematical and General*, **35(37)**: R31–150 (2002).
- [15] Mourik van, J., Saad, D., and Kabashima, Y., "Critical noise levels for low-density parity checking codes," *Phys. Rev. E*, **66**: 026705(1-8) (2002).
- [16] Takeda, K., and Nishimori, H., "Self-dual random-plaquette gauge model and quantum toric code," *Nucl. Phys. B*, **686**: 377–396 (2004).
- [17] Saika, Y., and Nishimori, H., "Statistical mechanics of image restoration using the plane rotator model," *J. Phys. Soc. Jpn.*, **71(4)**: 1052–1058 (2002).
- [18] Saika, Y., Inoue, J., Tanaka, H., and Okada, M., "Bayes-optimal solution of inverse halftoning based on statistical mechanics of the Q-Ising model," *Central Europ. J. Phys.*, **7(3)**: 444–456 (2009).
- [19] Saika, Y., and Aoki, T., "Thermodynamics-inspired inverse halftoning via multiple halftone images," *CAAI-Trans. Intell. Syst.*, **7(1)**: 86–94 (2012).
- [20] Saika, Y., and Nishimori, H., "Statistical mechanical approach to phase retrieval using the Q-Ising model," *Prog. Theor. Phys. Suppl.*, **157**: 292–295 (2005).